1 OF 1
AD
A046576

END
DATE
FILMED
12-77
DDC

1.0

1.1

1.25   1.4   1.6

2.8   2.5
3.2   2.2
2.0
1.8

MICROCOPY RESOLUTION TEST CHART
NATIONAL BUREAU OF STANDARDS-1963-A

REPORT DOCUMENTATION PAGE

READ INSTRUCTIONS
BEFORE COMPLETING FORM

1. REPORT NUMBER	2. GOVT ACCESSION NO.	3. RECIPIENT'S CATALOG NUMBER
4. TITLE (and Subtitle) Elastic and Inelastic Contributions to Secondary Electron Yield Structure		5. TYPE OF REPORT & PERIOD COVERED
		6. PERFORMING ORG. REPORT NUMBER
7. AUTHOR(s) M. L. den Boer, P. I. Cohen, Robert L. Park		8. CONTRACT OR GRANT NUMBER(s) N000-14-75-C-0292
9. PERFORMING ORGANIZATION NAME AND ADDRESS		10. PROGRAM ELEMENT, PROJECT, TASK AREA & WORK UNIT NUMBERS
11. CONTROLLING OFFICE NAME AND ADDRESS Dept. of Physics and Astronomy University of Maryland College Park, Maryland 20742		12. REPORT DATE Sep 77
		13. NUMBER OF PAGES 21 p.
14. MONITORING AGENCY NAME & ADDRESS(if different from Controlling Office) Office of Naval Research Physics Program Office Arlington, Va. 22217		15. SECURITY CLASS. (of this report) Unclassified
		15a. DECLASSIFICATION/DOWNGRADING SCHEDULE

16. DISTRIBUTION STATEMENT (of this Report)

DISTRIBUTION STATEMENT A
Approved for public release;
Distribution Unlimited

DDC
RECEIVED
NOV 17 1977
F

17. DISTRIBUTION STATEMENT (of the abstract entered in Block 20, if different from Report)

Approved for public release; distribution unlimited.

18. SUPPLEMENTARY NOTES

19. KEY WORDS (Continue on reverse side if necessary and identify by block number)

Secondary electron yield
Surface Physics
Appearance Potential Spectroscopy
Diffraction
Energy Distribution

20. ABSTRACT (Continue on reverse side if necessary and identify by block number)

The secondary electron yield of solid surfaces contains weak but complicated structure, which is greatly enhanced by differentiation with respect to primary electron energy. Auger electron appearance potential features, corresponding to yield changes due to core level excitations, and diffraction features are the major contributions to this structure. The magnitude of the diffraction features decreases with primary energy and depends strongly on temperature and surface order. Surprisingly, even for polycrystalline materials the diffraction features extend out to about 400 eV and completely obscure appearance (cont.)

DD FORM 1473 EDITION OF 1 NOV 65 IS OBSOLETE
1 JAN 73
S/N 0102-014-6601

AD A046576

AD No.
DDC FILE COPY

#20. Abstract, continued:

potential features in this region. ~~We have measured~~ the energy distribution
of electrons contributing to each of these kinds of features. The diffrac-
tion structure is due almost entirely to elastic electrons while the appear-
ance potential peaks result primarily from electrons with energy less than
30 eV. This difference can be exploited using a double modulation scheme
with 4 grid LEED optics to separate the two kinds of features. This extends
the useful range of Auger electron appearance potential spectroscopy down
to energies below 200 eV.

OFFICE OF NAVAL RESEARCH

Grant No. N000-14-75C-0292

ELASTIC AND INELASTIC CONTRIBUTIONS TO

SECONDARY ELECTRON YIELD STRUCTURE

by

M. L. den Boer, P. I. Cohen, Robert L. Park
Department of Physics and Astronomy
University of Maryland
College Park, Maryland 20742

ELASTIC AND INELASTIC CONTRIBUTIONS TO
SECONDARY ELECTRON YIELD STRUCTURE*

M. L. den Boer, P. I. Cohen, Robert L. Park
Department of Physics and Astronomy
University of Maryland
College Park, Maryland 20742

The secondary electron yield of solid surfaces contains weak but complicated structure, which is greatly enhanced by differentiation with respect to primary electron energy. Auger electron appearance potential features, corresponding to yield changes due to core level excitations, and diffraction features are the major contributions to this structure. The magnitude of the diffraction features decreases with primary energy and depends strongly on temperature and surface order. Surprisingly, even for polycrystalline materials the diffraction features extend out to about 400 eV and completely obscure appearance potential features in this region. We have measured the energy distribution of electrons contributing to each of these kinds of features. The diffraction structure is due almost entirely to elastic electrons while the appearance potential peaks result primarily from electrons with energy less than 30 eV. This difference can be exploited using a double modulation scheme with 4 grid LEED optics to separate the two kinds of features. This extends the useful range of Auger electron appearance potential spectroscopy down to energies below 200 eV.

Acknowledgments

Introduction

The secondary electron yield from electrons incident on solid sur-
faces has been studied for more than half a century. Plots of the yield
as a function of the incident electron energy contain an abundance of
small variations. In the low energy region these variations have been
attributed to diffraction effects,[1-3] and indeed their study has been
christened Low Energy Electron Reflection (LEER)[4] and Total Current
Spectroscopy (TCS).[5] Differentiation of the secondary electron yield
as a function of incident electron energy greatly enhances these diffrac-
tion features relative to the slowly varying background. In second
derivative plots, even from polycrystalline materials, the diffraction
effects have been shown to persist to several hundred electron volts.[6]

At higher incident energies additional structure has been observed
which has been identified with the thresholds for inelastic scattering
from atomic core states.[7] The study of these core excitations in the
total secondary yield, which is observed to increase at the thresholds,
is termed Auger Electron Appearance Potential Spectroscopy (AEAPS).[8]
When detected in the elastic yield, which decreases at the threshold,
the technique is termed Disappearance Potential Spectroscopy (DAPS).[9]
These techniques provide information about the local density of unfilled
states associated with each element in the surface region. Similar in-
formation is provided by Soft X-Ray Appearance Potential Spectroscopy
(SXAPS), in which the appearance potential is measured by detecting
changes in the photon yield. The major advantage of AEAPS and DAPS over

SXAPS is the reduction in primary current permitted by a larger signal and greater detection efficiency. Consequently, the sample heating and large current densities that can perturb weakly bound adsorbed layers are substantially reduced.

AEAPS and DAPS have been successfully used to study the electronic structure of a variety of materials with core binding energies above about 400 eV. However, unlike SXAPS, appearance potential signals at lower energies are obscured by the diffraction effects. For example, while the C 1s threshold at 284 V can easily be seen in SXAPS spectra of TiC, fig. 1 shows that in DAPS it is hidden by the diffraction. In addition, one would expect to observe fine structure extending several hundred electron volts above appearance potential thresholds similar to that found in extended X-ray absorption fine structure[10] and in SXAPS.[11] Indeed, with AEAPS or DAPS one should be able to examine structure above thresholds at energies not readily accessible to X-ray monochrometers. But first, the diffraction background must be removed.

Potentially, the diffraction features could be used to monitor structural changes on the surface of polycrystalline materials. In this paper, however, we will investigate the feasibility of separating the diffraction structure from the appearance potential features. In particular we will focus on the energy dependence of the electrons contributing to both sorts of structure.

Experimental

Experiments were performed in a Varian UHV system. Measurements were made with PHI 4-grid, hemispherical optics and a normal incidence electron gun. For the results to be presented here, Al(100), TiC(100), and polycrystalline Ti and Fe samples were used. These samples were cleaned by cycles of argon ion bombardment and annealing. Cleanliness was monitored with AES.

Changes in the total yield can be measured very simply by taking derivatives of the sample current.[12] In these experiments, however, we measure the collector current and use the grids to energy analyze the secondaries. To perform the differentiation, we modulate the accelerating potential by applying a 1V rms modulation between the sample and ground. In DAPS the first and last grids are grounded and the middle two retarding grids are set to pass only quasielastic electrons. In AEAPS, the first and last grids are set at a few volts positive to suppress background variations due to secondary emission from the grids. The middle two grids are set at the sample potential to pass all secondaries. The important point here is that when detecting quasielastic electrons, the retarding grid potential must be fixed with respect to the emitter potential. Otherwise, loss features will appear in the signal. Similarly, when the grids are set to pass all or all but low energy electrons, the retarding grids must be fixed with respect to the sample. Otherwise, as the sample potential is modulated, the proportion of the true secondary peak passed by the grids will be modulated and a spurious signal will be observed.

Results

The elastic and total yields from TiC(100) are shown in fig. 1. The structure in the elastic yield is much larger than the structure in the total yield, suggesting that only elastic electrons contribute to the diffraction features. This is of course what would be expected at very low incident energies, in which case most of the yield is elastic.[1,13] But at higher incident energies one might suppose that a decrease in the elastically scattered electrons would result in more inelastic excitations and an increase in the inelastic yield.

One sees the same sort of structure in the yields from polycrystalline materials and in fig. 2 we show spectra taken from polycrystalline Ti. Although the structure is much weaker, in the 2nd derivative plot it can be observed out to the Ti 2p appearance potential threshold.

To obtain the energy dependence of the electrons contributing to the diffraction structure we measured the second derivative of the scattered intensity at a series of analyzer grid voltages. At any grid voltage only those electrons with energy sufficient to pass the retarding grid contribute to the signal. For retarding potentials nearly equal to the incident accelerating voltage, the analyzer grids were fixed with respect to the filament to avoid modulating the characteristic loss features. For retarding potentials near zero the analyzer grids were fixed with respect to the sample to avoid similar artifacts due to the true secondary peak. The results are shown in fig. 3 in which the grid potential is always given referenced to the sample. At the highest grid potentials, in which case the analyzer to filament potential is small compared to the modulation amplitude, the signal represents the second derivative of the elastic

yield. As the grid to filament potential difference is increased to values larger than the modulation amplitude, the measured signal is still primarily the second derivative of the elastic yield. This is because the elastic peak, which dominates the collected current, is sharp relative to the grid to filament potential and modulation amplitude. Nevertheless, electrons suffering an inelastic loss may contribute once the retarding potential is sufficiently lowered. If a plasmon is created after an electron is elastically scattered[14] it will tend to enhance the diffraction structure. On the other hand, an electron that creates a plasmon before elastically scattering will tend to change the structure. The figure indicates that the diffraction contribution does not begin abruptly at the elastic peak but increases gradually as more electrons that have suffered losses are included in the collected signal. There is little change in the diffraction structure as the grid potential is further decreased. Even as the true secondary peak is included in the collected signal, little change in the diffraction structure is observed. This means that the intensity and shape of the true secondary peak does not change in a way comparable to the elastic intensity. Therefore, as far as the diffraction structure is concerned, both DAPS and AEAPS measure the derivative of only the elastic yield.

Fig. 3 also shows the energy distribution of electrons contributing to the Ti 2p appearance potential peak. With the analyzer potential set to pass only elastic electrons, the signal is the second derivative of the decrease in the elastic yield as the primary energy crosses the 2p threshold. As the potential is reduced, the signal becomes more negative

since plasmon loss replicas of the elastic beam are collected. When the threshold is crossed, these replicas decrease in the same way as the elastics. As the analyzer potential is decreased further, the signal represents roughly the increase in inelastic yield minus the decrease in elastic yield. The abrupt changes at 220 and 190 volts correspond to the inclusion of the Ti 2p Auger electrons which have left the sample without energy loss. At lower potentials there is a gradual increase in the signal as more inelastic electrons are included, until finally at around 20 V there is a very abrupt rise. This indicates that most of the inelastic electrons contributing to this particular appearance potential feature have energies less than about 20 eV.[15] These electrons are the decay products of excitations created by the 2p Auger electrons. This electron energy distribution is very different from the behavior observed for the diffraction features.

Fig. 4 shows the temperature dependence of several diffraction peaks in DAPS spectra from polycrystalline Fe and TiC (100). The Fe sample produces many visible diffraction spots, perhaps due to recrystallization during heating. The peak heights appear to decrease exponentially with increasing temperature even though many diffraction beams with different momentum transfers contribute. The peak heights of the TiC (100) sample exhibit no such simple dependence on temperature. This is to be expected since the thermal vibrations of two different kinds of atoms are involved. Since there is little decrease with increasing temperature, it is not possible in this case to reduce the diffraction effects, relative to appearance potential features, simply by heating.

The distinctly different energy distribution of electrons contributing to the diffraction and appearance potential features suggests an experimental procedure that would enhance the appearance potential features relative to the diffraction. By constructing a lowpass analyzer that just collects the electrons in the true secondary peak we would detect changes in the low energy yield due mainly to core hole excitations. We can simulate a bandpass analyzer by modulating the voltage of the retarding grid. This amounts to taking a derivative of the distribution shown in fig. 3 with respect to the retarding potential. One can see in this figure that at low retarding potentials the slope of the energy distribution curve for the appearance potential feature is much larger than that of the diffraction background. In practice we construct this pseudo-lowpass filter by modulating the retarding grid to sample potential between 0 and 10 V at a frequency f_1 = 20kHZ, the accelerating potential is modulated at a frequency f_2 = 13kHZ, and the component of collector current at $2f_2 - f_1$ is detected. We apply the modulation at frequency f_2 to the gun filament to avoid placing both modulations on the grids. Otherwise large background variations associated with secondary emission from the grids occur at the detection frequency. Consequently we must expect the background variations that occur when the gun operating conditions are modulated. The result for the TiC(100) sample is shown in fig. 5 where the bottom curve is a DAPS spectrum and the top curve is a measurement using the double modulation scheme. One can see that the magnitude of the diffraction features is reduced and that their shape is

Conclusion

EXAFS has been made surface sensitive by detecting the Auger elec-
trons that result from the decay of the X-ray excited core holes.[16] A
similar experiment could be imagined using electron excitation. However,
for a significant region above threshold, the fine structure will be
obscured by loss replicas of the elastic peak. This is because whenever
the elastic yield decreases, the loss replicas will follow suit. It
should be possible to look for much lower energy Auger electrons that
are far away from loss replicas. But then one could as well look at the
larger true secondary peak to obtain the same effect.

Unlike appearance potential features, a change in the elastic yield
is not reflected in the true secondary peak. Perhaps this is because
a decrease in the total backscattered intensity largely corresponds to
forward scattering to depths in the sample from which the electrons cannot
escape. The scatter in the data indicates that this is not completely
true, and especially at low incident energies one might expect that the
quasielastics would mix with the true secondaries. Certainly, our
results show that at incident energies above 60 eV, the elastic and
inelastic yield are remarkably decoupled.

To the extent that this decoupling holds, the diffraction features
can be removed from second derivative spectra by collecting only electrons
in the true secondary peak. However, we have not yet achieved the enhance-
ment that the different slopes of the curves in fig. 3 indicate possible
One difficulty stems from the slowly varying background that results from
modulation of the electron gun. Nevertheless, we have demonstrated that

AEAPS can be extended to lower incident energies than heretofore possible
and have found that the C 1s peak of TiC is much smaller in AEAPS than in
SXAPS.

References

1. I. H. Khan, J. P. Hobson, and R. A. Armstrong, Phys. Rev., 129, 1513 (1963).

2. M. G. Lagally, Ph. D. dissertation, University of Wisconsin, 1968 (unpublished).

3. P. E. Best, J. Appl. Phys., 45, 2351 (1974).

4. G. A. Haas, A. Shih, R. E. Thomas, Appl. Surf. Sci., (Sept., 1977).

5. S. A. Komolov and L. T. Chadderton, Rad. Eff., 31, 1 (1976).

6. R. L. Park, M. den Boer, Y. Fukuda, Proceedings of the 6th Czechoslovak Conference on Electronics and Vacuum Physics, 1976.

7. R. L. Gerlach, Surf. Sci., 28, 648 (1971).

8. J. E. Houston and R. L. Park, Phys. Rev. B, 5, 3808 (1972).

9. J. Kirschner and P. Staib, Phys. Rev. Lett., 42A, 335 (1973) and Appl. Phys. 6, 99 (1975).

10. F. W. Lytle, in Physics of Non-Crystalline Solids, ed. by J. A. Prins (North-Holland, Amsterdam, 1965) pp. 12-25; E. A. Stern, Phys. Rev. B, 10, 3027 (1974).

11. J. E. Houston and R. L. Park, J. Chem. Phys., 55, 4601 (1971).

12. Y. Fukuda, W. T. Elam, and R. L. Park, Phys. Rev. B, October 15, 1977.

13. E. G. McRae and C. W. Caldwell, Surf. Sci., 57, 63 (1976).

14. W. H. Weber and M. B. Webb, Phys. Rev., 177, 1103 (1969).

15. M. den Boer, P. I. Cohen and R. L. Park, to be published in Surf. Sci.

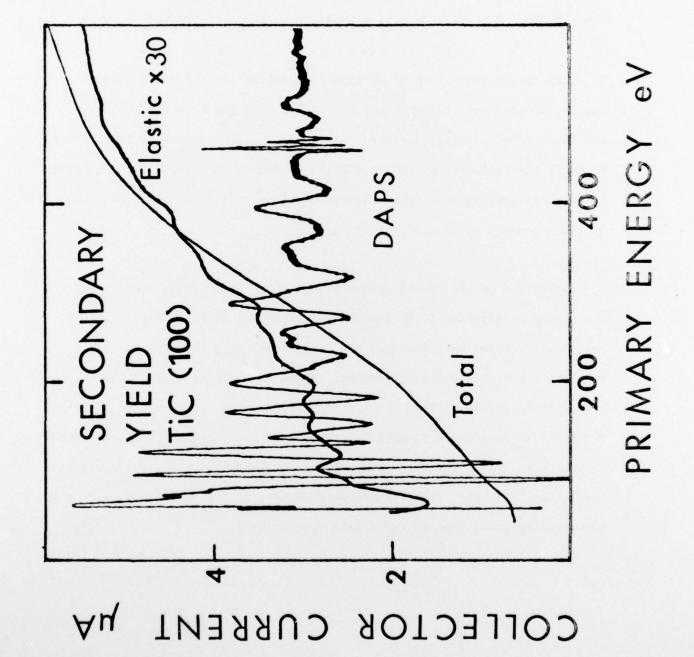16. H. Petersen and C. Kunz, Phys. Rev. Lett., 35, 863 (1975).

FIGURE CAPTIONS

1. Total yield and quasielastic yield of TiC (100) as a function of incident energy. The incident current increases monotonically with energy. Both total and elastic yield show changes with energy; these are much larger in the elastic yield. Also shown is the DAPS spectrum of TiC, which is the second derivative of the elastic yield with respect to incident energy. The units here are arbitrary. Differentiation enhances the diffraction features, and the Ti 2p and 2s appearance potential features become visible as well.

2. Total yield and quasielastic yield of polycrystalline Ti, taken as in fig. 1. The diffraction variations are now much smaller. Nevertheless, in the derivative, they extend out to the 2p edge if the gain is increased.

3. Energy dependence of electrons contributing to various features in the secondary yield of several different materials. These were obtained by taking the spectrum at a series of analyzer voltages. Curve a is the dependence of a peak in the Al (100) spectrum at 140 eV primary energy. Curve b is a peak at 110 eV from a polycrystalline Fe sample. Curves c, d, and e are all from TiC (100); c is a peak at 250 eV, d is a peak at 500 eV, and e is the Ti 2p appearance potential feature at 456 eV. The latter changes sign at 20 volts, indicating most of the electrons contributing to that signal are low energy electrons. In contrast, the diffraction peaks a through d change very little until the grid retarding voltage
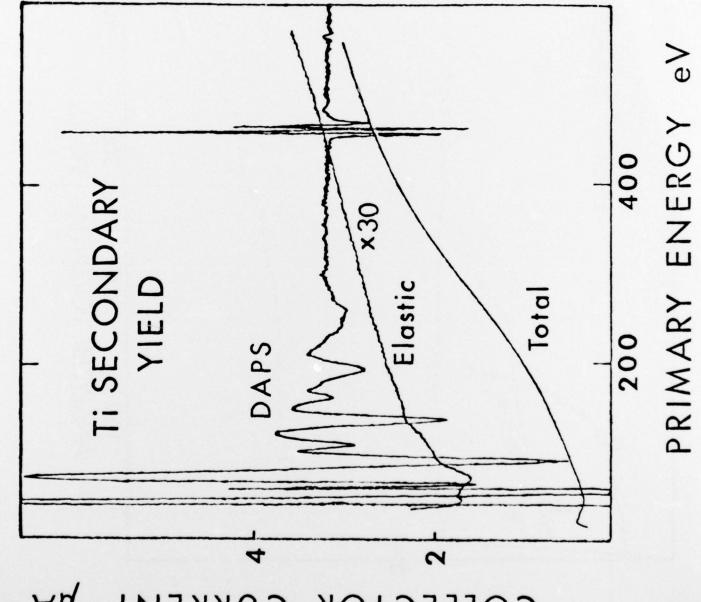
Figure Captions continued:

nears the accelerating potential. This indicates most of the electrons contributing to the diffraction signal are in the elastic beam.
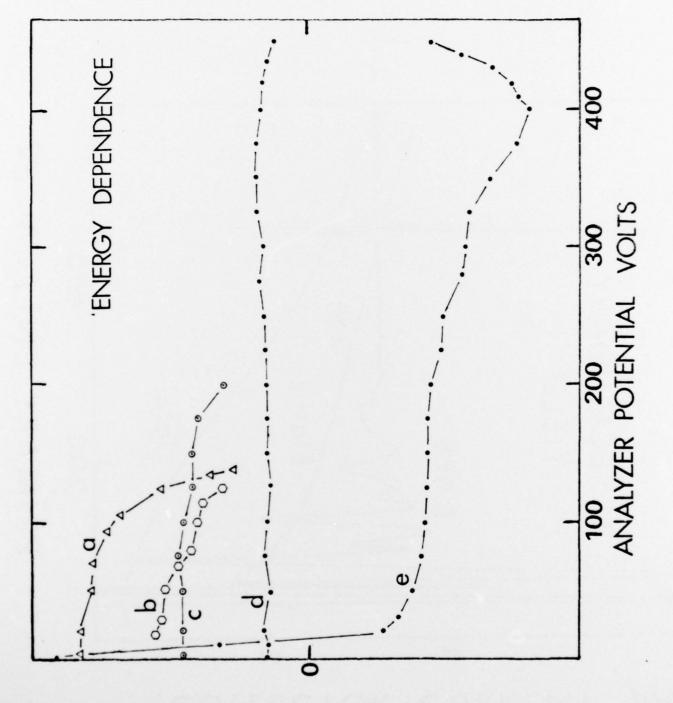
4. Temperature dependence of various features in the secondary yield spectra of polycrystalline Fe and TiC (100). The two Fe peaks at 53 eV and 95 eV primary energy decrease exponentially with increasing temperature. However, the TiC peaks at 110 eV and 180 eV change only slowly with temperature. This indicates it is not always possible to reduce diffraction effects in the secondary yield spectrum by heating.

5. Comparison of the second derivative of the elastic yield (DAPS) with the second derivative of the low energy, inelastic yield (upper spectrum). The slowly varying background in the upper curve is a consequence of modulating the electron gun filament. As we have shown, most of the electrons contributing to the diffraction features are elastic, while those contributing to an appearance potential feature have low energy. This is apparent in the upper curve (the derivative of the low energy, inelastic yield), in which the diffraction features are much weaker, relative to the appearance potential feature, than in the elastic yield (DAPS).
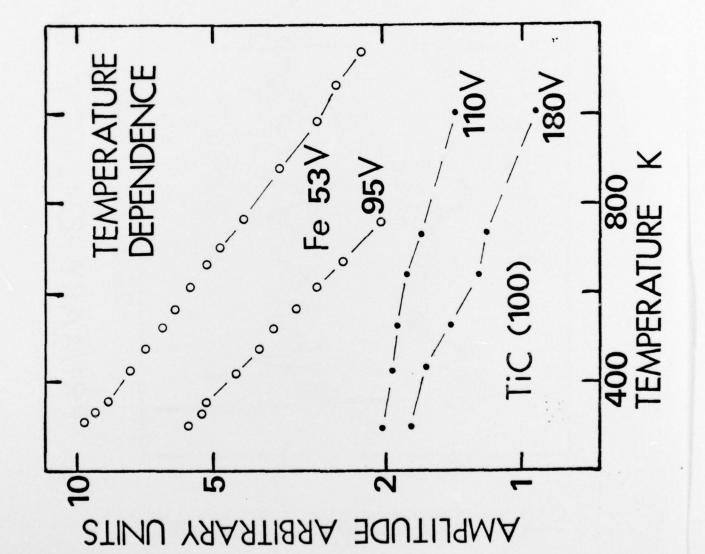
Ti SECONDARY YIELD

DAPS

x30

Elastic

Total

COLLECTOR CURRENT μA

4

2

PRIMARY ENERGY eV

200

400

ENERGY DEPENDENCE

AMPLITUDE ARBITRARY UNITS

ANALYZER POTENTIAL VOLTS

TEMPERATURE DEPENDENCE